

A 20, 1946 (1979).

<sup>2</sup>See, for example, A. Omont, *J. Phys. (Paris)* **26**, 26 (1965); P. R. Berman and W. E. Lamb, Jr., *Phys. Rev.* **187**, 221 (1969).

<sup>3</sup>T. Endo, T. Yabuzaki, M. Kitano, T. Sato, and T. Ogawa, *IEEE J. Quantum Electron.* **14**, 977 (1978).

<sup>4</sup>B. Decomps and M. Dumont, *J. Phys. (Paris)* **29**, 443 (1968).

### New Observation of Parity Nonconservation in Atomic Thallium

P. Bucksbaum, E. Commins, and L. Hunter

*Physics Department, University of California, Berkeley, California 94720, and Materials and Molecular Research Division, Lawrence Berkeley Laboratory, Berkeley, California 94720*

(Received 21 November 1980)

Refined observations of parity nonconservation in the  $6^2P_{1/2} - 7^2P_{1/2}$  transition in  $^{203,205}_{81}\text{Tl}$  are reported. Absorption of circularly polarized 293-nm photons by  $6^2P_{1/2}$  atoms in an  $E$  field results in polarization of the  $7^2P_{1/2}$  state, through interference of the Stark  $E1$  amplitude with  $M1$  and parity-nonconserving  $E1$  amplitudes. Detection of this polarization yields the circular dichroism  $\delta = +(2.8 \pm 0.9) \times 10^{-3}$ , which agrees with theoretical estimates based on the Weinberg-Salam model, for  $\sin^2 \theta_W = 0.23$ .

PACS numbers: 32.90.+a, 11.30.Er, 12.30.Cx

We report new observations of parity nonconservation (PNC) in the  $6^2P_{1/2} - 7^2P_{1/2}$  transition in atomic thallium (see Fig. 1). The transition amplitude is forbidden  $M1$  with measured amplitude  $\mathfrak{M} = (-2.1 \pm 0.3) \times 10^{-5} |e\hbar/2m_e c|$ .<sup>1</sup> Parity nonconservation causes the  $6^2P_{1/2}$  and  $7^2P_{1/2}$  states to be admixed with  $^2S_{1/2}$  states; thus the transition amplitude contains an additional  $E1$  component  $\mathcal{E}_p$ . This results in circular dichroism, defined by

$$\delta = \frac{\sigma_+ - \sigma_-}{\sigma_+ + \sigma_-} = \frac{2 \operatorname{Im}(\mathcal{E}_p \mathfrak{M}^*)}{|\mathfrak{M}|^2 + |\mathcal{E}_p|^2} \approx \frac{2 \operatorname{Im} \mathcal{E}_p}{\mathfrak{M}}, \quad (1)$$

where  $\sigma_{\pm}$  are the cross sections for absorption of 293-nm photons, with  $\pm$  helicity, respectively. Theoretical estimates of  $\mathcal{E}_p$  based on the Weinberg-Salam (W-S) model<sup>2</sup> yield<sup>3-5</sup>

$$\begin{aligned} \delta_{\text{theor}} &= 2 \operatorname{Im}(\mathcal{E}_{p,\text{theor}})/\mathfrak{M}_{\text{expt}} \\ &= (2.1 \pm 0.7) \times 10^{-3} \end{aligned} \quad (2)$$

for  $\sin^2 \theta_W = 0.23$ , where  $\theta_W$  is the Weinberg angle.

The aim of this experiment is to measure  $\delta$ . The dipole amplitudes  $\mathcal{E}_p$  and  $\mathfrak{M}$  are observed by their interference with a Stark  $E1$  amplitude  $\beta E$  caused by a 215-V/cm electric field  $E$ , in the  $6P_{1/2}, F=0 - 7^2P_{1/2}, F=1$  transition. This causes a polarization  $\Delta = -(2\mathfrak{M}/\beta E)(1 \pm \frac{1}{2}\delta)$  in the  $7^2P_{1/2}, F=1$  state. The latter is analyzed by selective excitation of  $m_F = +1$  or  $-1$  substates to the  $8^2S_{1/2}$  state with circularly polarized 2.18- $\mu\text{m}$  light, followed by observation of  $8^2S_{1/2} - 6^2P_{3/2}$  fluorescence at 323 nm. (See Fig. 1.) In a preliminary version of the experiment<sup>6</sup> we obtained the result

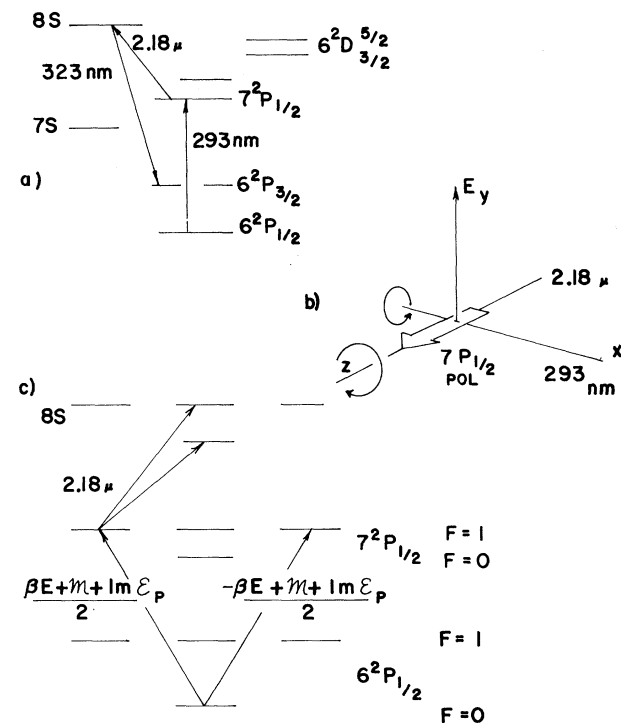


FIG. 1. (a) Low-lying energy levels of Tl (not to scale). (b) Coordinate system, orientation of photon beams, and electric field direction. (c) Schematic diagram indicating production and analysis of  $7^2P_{1/2}$  polarization in the 0-1 transition. The transition amplitudes to the  $m_F = \pm 1$  levels of  $7^2P_{1/2}$  are indicated. The polarization is analyzed by circularly polarized 2.18- $\mu\text{m}$  radiation ( $7^2P_{1/2} - 8^2S_{1/2}$  transition). The  $8^2S_{1/2}$  hfs is not resolved.

$\delta = +(5.2 \pm 2.4) \times 10^{-3}$ . Although the basic method has remained unchanged, numerous improvements in the apparatus have been made and we have also carried out a thorough investigation of possible sources of systematic error.

Apparatus improvements include use of a new thallium cell with better geometry, yielding higher signal and lower background; better detection efficiency; better laser stability and higher laser output power; use of a Pockels cell instead of a rotating quarter-wave plate to produce circularly polarized 293-nm light; automatic laser frequency control for 293 nm light; use of a faster on-line computer with a more sophisticated interface and running program; use of a mirror to reflect the 293-nm beam back through the main cell, which does not affect the genuine parity asymmetry but reduces the  $M1$  asymmetry; and

other miscellaneous improvements.

The main sources of possible systematic error (false parity asymmetry) are (A) imperfect uv circular polarization and (B) stray fields in the interaction regions which do not reverse exactly in proportion to the main component of electric field employed in the Stark effect.<sup>7</sup> Effects of type A arise from dilution of the  $M1$  asymmetry  $\Delta_M = -2\mathfrak{M}/\beta E$  by uv polarization-dependent admixtures of 0-0 intensity and background in the 0-1 line, as well as slight dependence of reflections on uv polarization when the mirror is used (unblocked). It can be shown that, for case A, the false parity asymmetry for mirror not used (blocked, subscript  $b$ ) is

$$\Delta_b^A = \left( \frac{1+f}{1-f} \right) \Delta_{Mb} \left[ \frac{B_b}{S_b} (\Gamma_b - \Gamma_u) + \frac{2f}{1+f} \Gamma_b \right] \quad (3)$$

while for mirror unblocked (subscript  $u$ ) it is

$$\Delta_u^A = \left( \frac{1+f}{1-f} \right) \Delta_{Mb} \frac{(S+B)_b}{S_b(S+B)_u} \left[ 2(S+B)_b (\Gamma_b - \Gamma_u) + 2B_B (\Gamma_u - \gamma_b) + B_u (\gamma_u - \Gamma_u) + \frac{2f}{1+f} (2S_b - S_u) \gamma_u \right]. \quad (4)$$

Here  $S$  and  $B$  are signal and background, respectively;  $\Delta_M$  is the observed  $M1$  asymmetry,  $f = S_{00}/S_{01} = 0.09$ ,  $\gamma = (B_L - B_R)/(B_L + B_R)$ , and  $\Gamma = [(S+B)_L - (S+B)_R]/[(S+B)_L + (S+B)_R]$ , where  $L$  and  $R$  correspond to  $\pm$  uv helicities, respectively. For case B, the false parity asymmetry is

$$\Delta^B = -2 \frac{E_{0x} \Delta E_z}{E_{0y}^2} - 2 \frac{\Delta E_x E_{0z}}{E_{0y}^2} + 4 \frac{E_{0x} E_{0z} \Delta E_y}{E_{0y}^3}, \quad (5)$$

where  $\vec{E}_\pm = \pm \vec{E}_0 + \Delta \vec{E}$ , the coordinates are as defined in Fig. 1(b), and  $E_{0y}$  is the main, reversing component of electric field. Finally, there is a false parity asymmetry arising from a combination of effects A and B:

$$\Delta^{AB} = - \frac{2\mathfrak{M}}{E_{0y} \beta} \frac{E_{0z}}{E_{0y}} (\eta \sin \varphi + \eta' \sin \varphi'), \quad (6)$$

where the actual uv circular polarization states  $R$  and  $L$  are expressed in terms of the nominal states  $\hat{e}_R = (\hat{y} - i\hat{z})/\sqrt{2}$  and  $\hat{e}_L = (\hat{y} + i\hat{z})/\sqrt{2}$  by

$$\hat{R} = (1 - \eta^2)^{1/2} \hat{e}_R + \eta e^{i\varphi} \hat{e}_L, \quad (7)$$

$$\hat{L} = (1 - \eta'^2)^{1/2} \hat{e}_L + \eta' \exp(i\varphi') \hat{e}_R. \quad (8)$$

Formulas (3)–(6) have the great advantage that all quantities on their right-hand sides are determined experimentally with precision. The quantities in (3) and (4) are measured simultaneously with all parity data, and those in (5) and (6) are measured by a series of auxiliary experiments performed very frequently during each parity run. These involve asymmetry measurements with linearly polarized uv, and with circularly

polarized uv and a magnetic field of  $\pm 5$  G along the beam direction. All such measurements are done with and without the mirror. The measurements for Eqs. (3) and (4) automatically provide a precise correction for 0-0 dilution and render unnecessary a separate measurement of the 0-0 parity asymmetry, which was required in our earlier work.<sup>6</sup> Corrections for effects A and AB depend on Pockels cell and mirror alignment to some extent, and there is no indication of variation between alignments. Effects B are very consistent from run to run.

The data on which our present result is based were taken in 11 separate runs ( $\sim 400$  h total). Approximately  $8.7 \times 10^6$  laser pulses were devoted to the  $6^2P_{1/2}, F=0 - 7^2P_{1/2}, F=1$  (0-1) transition with the mirror, and  $5.2 \times 10^6$  pulses to the 0-1 transition without the mirror. These were interspersed in groups of 2048 and 1024 pulses, respectively. An additional  $6 \times 10^6$  pulses were devoted to background and systematic measurements. Observations of the  $M1$  and parity asymmetries were carried out simultaneously. Data were also obtained for the 0-0 transition, which should not and does not display parity violation.

The results are summarized in Table I. Column 2 gives the average  $M1$  asymmetry observed for each run. It fluctuates because of variable dilutions from background, variable small admixtures of 0-0 signal, and imperfections in 2.18- $\mu$ m polarization. Since these dilutions affect the

TABLE I. Summary of asymmetry results.

Run	Observed	Corrected	
	$M1$ asymmetry $\Delta_M$ (No mirror)	parity asymmetries normalized to $\Delta_M = 9.0 \times 10^{-3}$	
		$\Delta_{p1}$ (Mirror)	$\Delta_{p2}$ (No mirror)
1	$6.40 \times 10^{-3}$	$1.06 \pm 1.97 \times 10^{-5}$	$-0.16 \pm 3.15 \times 10^{-5}$
2	$7.26 \times 10^{-3}$	$2.54 \pm 2.05 \times 10^{-5}$	$0.17 \pm 2.56 \times 10^{-5}$
3	$6.94 \times 10^{-3}$	$-0.82 \pm 2.86 \times 10^{-5}$	$6.07 \pm 4.83 \times 10^{-5}$
4	$7.04 \times 10^{-3}$	$-0.20 \pm 1.53 \times 10^{-5}$	$4.48 \pm 2.36 \times 10^{-5}$
5	$6.90 \times 10^{-3}$	$3.45 \pm 1.88 \times 10^{-5}$	$1.18 \pm 3.37 \times 10^{-5}$
6	$7.54 \times 10^{-3}$	$-1.65 \pm 2.05 \times 10^{-5}$	$-3.50 \pm 4.03 \times 10^{-5}$
7	$7.15 \times 10^{-3}$	$0.93 \pm 1.13 \times 10^{-5}$	$0.75 \pm 2.02 \times 10^{-5}$
8	$7.24 \times 10^{-3}$	$2.07 \pm 0.84 \times 10^{-5}$	$2.34 \pm 1.13 \times 10^{-5}$
9	$6.31 \times 10^{-3}$	$-0.27 \pm 2.27 \times 10^{-5}$	$-0.83 \pm 3.48 \times 10^{-5}$
10	$6.83 \times 10^{-3}$	$2.28 \pm 2.10 \times 10^{-5}$	$-1.62 \pm 2.86 \times 10^{-5}$
11	$6.81 \times 10^{-3}$	$3.65 \pm 1.46 \times 10^{-5}$	$2.25 \pm 1.99 \times 10^{-5}$
Weighted averages <sup>a</sup>		$1.43 \pm 0.45 \times 10^{-5}$ a	$1.55 \pm 0.58 \times 10^{-5}$ a

<sup>a</sup>Averages computed from binning of above data into 425 separate groups. Prior to correction of parity data for stray electric field and polarization effects,  $\Delta_{p1} = +0.93 \times 10^{-5}$  and  $\Delta_{p2} = +1.18 \times 10^{-5}$ .

parity and  $M - 1$  polarizations equally, we arbitrarily normalize the parity asymmetries  $\Delta_p$  to an  $M1$  asymmetry  $\Delta_M$  for no mirror of  $9.0 \times 10^{-3}$  (column 3). The uncertainties for  $\Delta_p$  are in each case compounded from the statistical uncertainties in the data and in the systematic corrections. The weighted averages of the normalized parity asymmetries with and without the mirror are respectively

$$\Delta_{p,1} = (1.46 \pm 0.45 \pm 0.11) \times 10^{-5}, \quad (9)$$

$$\Delta_{p,2} = (1.58 \pm 0.58 \pm 0.06) \times 10^{-5}. \quad (10)$$

The first uncertainty in Eqs. (9) and (10) is statistical, the second is a nonstatistical uncertainty dominated by correction A. Corrections for effects A amount to  $5.7 \times 10^{-6}$  for the unblocked case and  $1.4 \times 10^{-6}$  for the blocked case. The uncertainties, mainly systematic, are less than 20% of the corrections  $\Delta_{u,b}^A$ . Corrections for effect AB are very small. As for correction B, typically  $E_{0x}/E_{0y} \sim 10^{-2}$ ,  $E_{0x}/E_{0y} \sim 2 \times 10^{-3}$ ,  $\Delta E_x/E_{0y} \sim 4 \times 10^{-4}$ ,  $\Delta E_x/E_{0y} \sim 10^{-4}$ , and  $\Delta E_y/E_{0y} \sim 2 \times 10^{-3}$ . The uncertainty in  $\Delta^B$ , mainly statistical, is less than  $5 \times 10^{-7}$ . Results (9) and (10) are consistent and their weighted average is

$$\Delta_p(0-1) = (1.51 \pm 0.36 \pm 0.09) \times 10^{-5}. \quad (11)$$

To obtain  $\delta = 2 \text{Im}(\mathcal{E}_p)/\Re$  we take the ratio  $2\Delta_p(0-1)/\Delta_{M'}$ , where  $\Delta_{M'} = K \times 9.0 \times 10^{-3}$ . The factor  $K$

corrects for reflections from the rear of the main cell, which reduces  $\Delta_M$  but not  $\Delta_p$ . We estimate  $K = 1.17$ , but it might be somewhat less which leads to a skewness in the systematic uncertainty of our final result. The latter is

$$\delta = +(2.8 \pm 0.7_{-0.2}^{+0.3}) \times 10^{-3}, \quad (12)$$

which is consistent with  $\delta_{\text{theor}}$  [see Eq. (2)]. Our result may be expressed in terms of the weak charge  $Q_W$ , defined in the Weinberg-Salam model as

$$Q_W = Z(1 - 4 \sin^2 \theta) - N = -116$$

for  $\sin^2 \theta_W = 0.23$ . We find

$$Q_{W,\text{expt}} = -155 \pm 63. \quad (13)$$

A full report of this research, including a detailed account of systematic effects, has been prepared for publication.

We thank S. Chu, R. Conti, and D. Neuffer for their invaluable collaboration in the early phases of this work, P. Drell for many discussions and useful assistance, and glassblowers D. Anderberg and R. Hamilton for excellent workmanship. This research was done under the auspices of the Chemical Sciences Division, Office of Basic Energy Sciences, U. S. Department of Energy.

<sup>1</sup>S. Chu, E. Commins, and R. Conti, Phys. Lett. **60A**,

96 (1977).

<sup>2</sup>S. Weinberg, Phys. Rev. Lett. **19**, 1264 (1967), and **27**, 1688 (1971), and Phys. Rev. D **5**, 1412 (1972);A. Salam, in *Elementary Particle Theory*, edited by N. Svartholm (Almqvist Forlag, Stockholm, 1968).<sup>3</sup>D. V. Neuffer and E. Commins, Phys. Rev. A **16**, 844 (1977).<sup>4</sup>O. P. Sushkov, V. V. Flambaum, and I. B. Khriplovich, Pis'ma Zh. Eksp. Teor. Fiz. **24**, 461 (1976) [JETP Lett. **24**, 502 (1976)].vich, Pis'ma Zh. Eksp. Teor. Fiz. **24**, 461 (1976) [JETP Lett. **24**, 502 (1976)].<sup>5</sup>B. P. Das, J. Andriessen, S. N. Ray, Mina Vajed-Samii, and T. P. Das, to be published.<sup>6</sup>R. Conti, P. Bucksbaum, S. Chu, E. Commins, and L. Hunter, Phys. Rev. Lett. **42**, 343 (1979).<sup>7</sup>M. A. Bouchiat, J. Guená, and L. Pottier, J. Phys. (Paris), Lett. **41**, L299 (1980).

## Measurement of Parity Nonconservation in Atomic Bismuth

J. H. Hollister, G. R. Apperson,<sup>(a)</sup> L. L. Lewis,<sup>(b)</sup> T. P. Emmons, T. G. Vold, and E. N. Fortson*Department of Physics, University of Washington, Seattle, Washington 98195*

(Received 23 December 1980)

Parity-nonconserving optical rotation has been observed and measured on the 8757-Å magnetic-dipole absorption line in atomic bismuth vapor. The result,  $R \equiv \text{Im}(E_1/M_1) = (-10.4 \pm 1.7) \times 10^{-8}$ , is of the approximate size calculated with use of the Weinberg-Salam theory of the weak neutral-current interaction with  $\sin^2\theta_W = 0.23$ .

PACS numbers: 32.90.+a, 12.20.Hx, 12.30.Cx, 42.10.Nh

We report here the result of a series of measurements of optical rotation in atomic bismuth vapor at the 8757-Å magnetic-dipole absorption line. The appearance of parity-nonconserving (PNC) optical rotation induced by the weak neutral-current interaction between the atomic electrons and nucleons is a significant prediction of the Weinberg-Salam theory<sup>1,2</sup> of weak interactions. The effect is largest in heavy atoms.<sup>3,4</sup> Our measurements reveal a well-resolved optical rotation that agrees in sign and approximate magnitude with recent calculations of the effect in bismuth based on the Weinberg-Salam theory.

Since the time of our earliest measurements<sup>5,6</sup> on this bismuth line, which were not mutually consistent, we have added a new laser, improved the optics, and included far more extensive systematic checks. Our present result (see Table I below) is based on many separate measurements made over the past two years (data collection periods I-V), all in good agreement with each other.

Although a PNC neutral-current interaction between electrons and nucleons in agreement with the Weinberg-Salam theory has been observed in high-energy electron scattering,<sup>7</sup> the situation in atoms is unclear. Our experiment and the bismuth optical-rotation experiments by three other groups<sup>8-10</sup> have yielded results with significant mutual discrepancies far larger than quoted errors. The overall evidence possibly favors some PNC effect in bismuth,<sup>4</sup> and similar evidence about thallium comes from measurements at

Berkeley of circular dichroism in thallium vapor.<sup>11</sup>

We determine the quantity  $R \equiv \text{Im}(E_1/M_1)$ , where  $M_1$  is the magnetic-dipole amplitude of the absorption line and  $E_1$  is the electric-dipole amplitude coupled into the same line by the PNC interaction between the atomic electrons and nucleons. The two dipoles combine to produce a rotation of the plane of polarized light in bismuth vapor by an angle  $\varphi_{\text{PNC}} = -4\pi l \lambda^{-1} (n-1)R$ , where  $n$  is the refractive index due to the magnetic-dipole line,  $\lambda$  is the wavelength, and  $l$  the path length. Sharp dispersive changes in  $\varphi_{\text{PNC}}$  at each hyperfine component of the line help to distinguish the signal from background rotations.

The plan of the experiment is shown in Fig. 1. A tunable laser beam passes through a calcite-prism polarizer, a water-filled Faraday cell, a heated bismuth cell, and a second polarizer crossed with the first; and then enters a silicon *p-i-n* photodiode detector. Light reflected from the front surface of the second polarizer is detected as a reference signal to divide out intensity variations. Both Nicol and Glan-Thompson polarizers have been used.

The Faraday cell produces a sinusoidal rotation of the plane of polarization with a frequency of 1 kHz and an amplitude of about  $10^{-3}$  rad. Any rotation of the plane of polarization in the bismuth cell is measured by phase-sensitive detection (PSD) of the 1-kHz component from the signal detector. The PSD output, together with other signals for use in the analysis, is stored in a PDP-